Palestine Journal of Mathematics

Vol. 7(1)(2018) , 167–190

A Numerical Solution Technique for Solving an Inverse Eigenvalue Problem of Computing Guided Modes in a Class of Optical Fibers

Hayat REZGUI and Abdelaziz CHOUTRI

Communicated by S. Khoury

MSC 2010 Classifications: Primary 65F18, 35Q60; Secondary 46N10, 52A41, 78M10.

Keywords and phrases: Inverse eigenvalue problems, optical fibers, graded-index refraction, convex optimization, *Lagrange* multipliers.

Abstract This paper describes a numerical technique for determining the best approximation of the exact refractive index (of an optical fiber having a circular cross section), allowing a better transmission of a given information. Mathematically, this objective leads to the resolution of an inverse eigenvalue problem that consists in reconstructing the refractive index from a prescribed finite set of eigen data (of the direct problem), knowing only the wavenumber in vacuum (the frequency). The corresponding direct problem (solved by a finite element method) consists of computing guided modes that propagate, under weak guidance assumptions, in a graded-index optical fiber with a circular-shaped section. The numerical resolution of the inverse problem is due to a special Algorithm for solving a convex optimization problem using *Lagrange* multipliers. Examples and numerical illustrations, related to the inverse problem, show the robustness and the higher efficiency obtained by our suggested method that converges geometrically to the exact refractive index.

1 Introduction

Optical fibers are one of the perfect physical environment and important scientific achievements in the last century [1] and they are certainly of considerable interest because they represent the best current way to transport very high debits of digital information. The needs in this area are likely to increase very strongly in the near future [18, 57]. It is by this means that circulate over 80% of global long distance traffic information. The idea of using optical fibers to transmit information [57] appeared in the early 60s with the appearance of Laser, and the advantages of transmitting information [18, 46, 57] by optical fibers are multiple compared to other communication media [25] (one pair of optical fibers carries a rate of 10 times stronger than 250 pairs of copper wires). Thanks to comfort and energy saving provided by optical fibers, these last are perfect for medical applications, the lighting field, the road transport system and for various military applications requiring a high quality equipment.
In this paper, we limit ourselves on optical fibers of famous profile class so-called power-law-profiles (graded-index profiles) [14, 18, 21, 39, 42, 46, 57, 61].
The aim of this work is to exhibit a numerical method (based on a constrained convex optimization procedure [8, 10, 17, 47, 60]) to determine a suitable approximation of the refractive index (of the considered optical fiber), which allows a better transmission of a given information.
Consequently, we are interested in solving an inverse eigenvalue problem [3, 4, 5, 11, 12, 26, 40], of computing guided modes [36, 52] (the direct problem) that propagate under weak guidance assumptions [15, 16, 18, 36, 42, 46, 52], in an optical fiber with a circular cross section (Figure 1), and a graded refractive index [42] (α-power refractive-index (Figure 2), (Figure 3) and (Figure 4)) whose radial refractive-index profile n (which is a real function of two real variables x

and y) has the form [15, 46, 48, 57]:

$$\begin{aligned} n(x,y) &= \begin{cases} n_+\sqrt{1-2\delta\left(\frac{r}{a}\right)^{\alpha}} & ,0 \le r = \sqrt{x^2+y^2} \le a \\ n_\infty & ,\text{otherwise} \end{cases} \\ &= n(r) \end{aligned}$$

where

$$\begin{cases} n \in L^\infty(\mathbb{R}^2),\ n_+ = \sup\limits_{(x,y)\in\mathbb{R}^2} n(x,y),\ n_+ > n_\infty > 0, \\ \delta = \dfrac{n_+^2 - n_\infty^2}{2n_+^2},\ (\delta \ll 1,\ \delta \text{ is the normalized difference index}), \\ 1 \le \alpha \text{ is the profile parameter, it determines the shape of the core's profile}, \\ r \text{ is the radial component and } a \text{ is the characteristic radius of the fiber's core.} \end{cases}$$

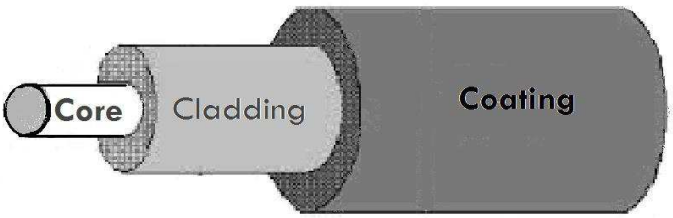

Figure 1: An optical fiber (with a circular cross section)

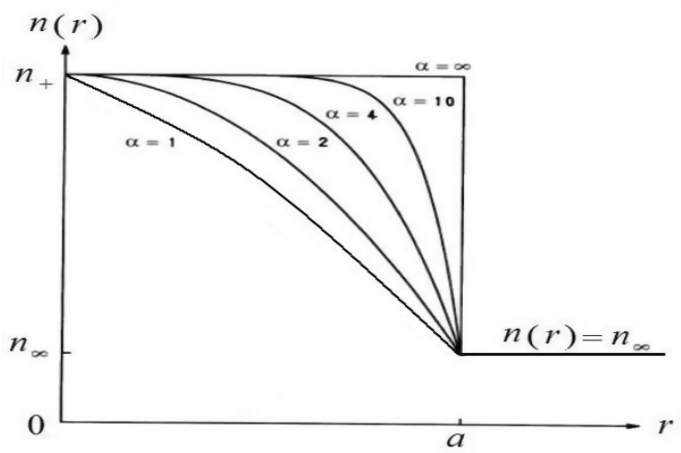

Figure 2: Potential of a graded-index profile for different exponents α ($\alpha \ge 1$)

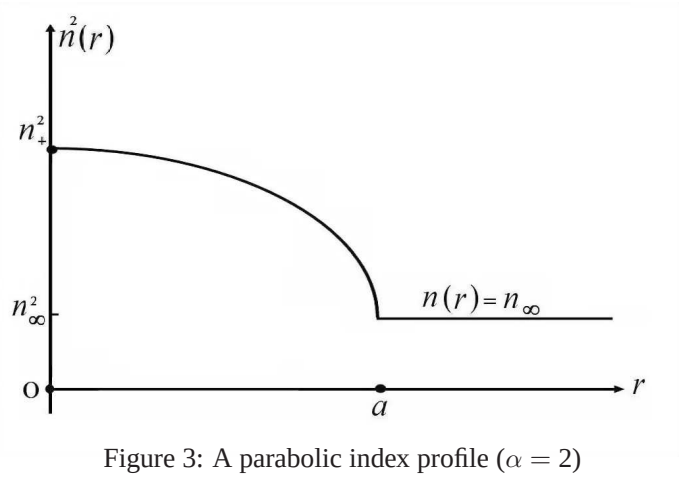

Figure 3: A parabolic index profile ($\alpha = 2$)

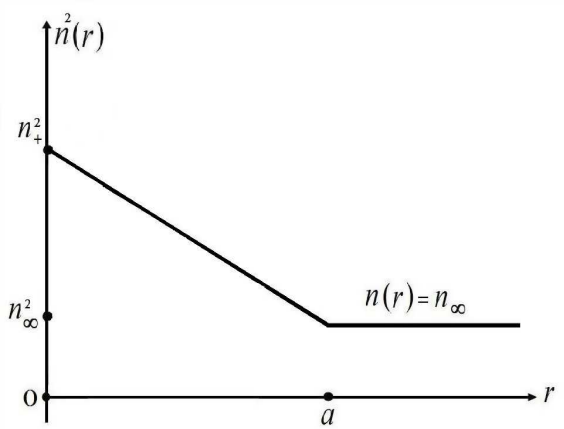

Figure 4: A triangular (linear) index profile ($\alpha = 1$)

1.1 Brief overview of previous works [49]

Several publications have appeared in recent years documenting the measurement of dielectric constant (relative permittivity) or the reconstruction of refractive indices, for example:

- Numerical reconstruction of the variable refractive index of multi-layered circular weakly guiding dielectric waveguides using the measurements of the propagation constants of their eigenwaves (see [29]).
- Universal numerical methods for reconstruction of refractive indices of dielectric objects designed for coefficient inverse diffraction problems (see [6]).
- The methods for determination of the optical characteristics of dielectric waveguides proposed for waveguides of some special forms (see [54], [55]).
- Approximation W.K.B. used in planar waveguides for the determination of index profile (see [37]).
- The waveguide spectroscopy widely used for planar (one-dimensional) multi-layered waveguides (see [31]).
- This last method was extended to the two-dimensional problem for the waveguide with the piecewise-constant refractive index and an arbitrary cross-sectional boundary (see [28], [30]).

- A method is described for determining unambiguously, from the far-field pattern of single mode fibers, the core diameter and the refractive-index difference between core and cladding (see [20]).
- A simple and rapid method is described for determining the refractive-index profile of an optical fiber by the observation of the near-field intensity distribution (see [53]).

The refractive-index distribution in an optical fiber is fundamental in determining its transmission properties, it is usually inferred from preform measurements.
The objective of this paper is to reconstruct the refractive-index (as a function of the radial component) of an optical fiber having a graded-index profile and a circular cross section.
In this paper, we limit ourselves to stating the results obtained through the numerical process adopted in this work with a discussion and a lot of accompanied commentary and remarks.

2 The Mathematical Model

Computing guided modes in optical fibers under weak guidance assumptions is equivalent to solve the following eigenvalue problem (Π) posed in the whole plane $\mathbb{R}^2$ [15, 16, 48]:

$$(\Pi)\left|\begin{array}{l}\text{Find } \lambda \in \left]0, V^2\right[, u \in H^1(\mathbb{R}^2),\ u \neq 0 \text{ , such that:}\\ \\ -\Delta u + q(x,y)u = -\lambda u, \text{ in } \mathbb{R}^2\end{array}\right.$$

where

$$\begin{aligned} q(x,y) = -k^2(n^2(x,y) - n_\infty^2) &= -k^2(n^2(r) - n_\infty^2) \\ &= \begin{cases} -V^2(1 - \left(\frac{r}{a}\right)^\alpha) & ,0 \leq r \leq a \\ 0 & ,a \leq r \end{cases} \\ &= q(r) \end{aligned} \tag{2.1}$$

and

$$\begin{cases} \Delta \text{ is the Laplacian operator in 2 dimensions,} \\ \lambda \text{ is an eingenvalue of the direct problem } (\Pi), \\ k \text{ is the wavenumber in vacuum (frequency), it is assumed to quite large,} \\ V^2 = k^2(n_+^2 - n_\infty^2), V \text{ is the normalized frequency,} \\ u \text{ is a transverse component of the electromagnetic field.} \end{cases}$$

We note that solving the direct problem (Π), using a finite element method [23, 35, 43, 51], consists in calculating the couples (λ, u), but the finite element approximation is not however suitable for solving the problem (Π) because of the unboundedness of the domain $\mathbb{R}^2$, so, we first reduce (Π) to a bounded domain as follows [15, 48]:

$$(\Pi')\left|\begin{array}{l}\text{Find } \lambda_R \in \left]0, V^2\right[, u_R \in H^1(\Omega_R), u_R \neq 0 : \\ \\ -\Delta u_R + q(x,y)u_R = -\lambda_R u_R, \text{ in } \Omega_R \\ \\ \gamma_1 u_R + \gamma_2 \dfrac{\partial u_R}{\partial r} = g, \text{ on } S_R\end{array}\right.$$

such that

$$\begin{cases} \lambda_R \text{ is an eigenvalue of the direct problem } (\Pi'), \\ \mathbf{\Omega}_R = \left\{(x,y) \in \mathbb{R}^2 \,/\, x^2+y^2 < R^2\right\}, S_R = \left\{(x,y) \in \mathbb{R}^2 \,/\, x^2+y^2 = R^2\right\}, \\ S_R \text{ is the artificial boundary, it encloses the optical fibre's core defined by :} \\ \mathbf{\Omega}_a = \left\{(x,y) \in \mathbb{R}^2 \,/\, x^2+y^2 < a^2\right\}, \text{thus } R \text{ must satisfy: } 0 < a < R, \\ \gamma_1, \gamma_2 \in \mathbb{R},\ \gamma_1 \text{ and } \gamma_2 \text{ cannot vanish at the same time}, \\ g \text{ is a real function defined on } S_R, \\ \dfrac{\partial u_R}{\partial r} \text{ denotes the exterior normal derivative of } u_R \text{ along } S_R. \end{cases}$$

3 The Inverse Eigenvalue Problem

The inverse eigenvalue problem to be solved (in this work) is:

$$(\Pi'') \left| \begin{array}{l} \text{Find } q \in L^\infty(\mathbf{\Omega}_R), \text{ such that :} \\ \\ -\Delta u(x,y) + q(x,y)u(x,y) = -\lambda u(x,y), \text{ in } \mathbf{\Omega}_R \end{array} \right.$$

knowing only:

(i) The frequency k.

(ii) A finite number of spectral data (λ, u) (associated to a certain boundary condition: Dirichlet, Neumann, Robin,...) of the direct problem (Π').

Communication implies transfer of information from one point to another. When it is necessary to transmit information, such as speech, images, or data, over a distance, one generally uses the concept of carrier wave communication. In such a system, the information to be sent modulates an electromagnetic wave such as a radio wave, microwave, or light wave, which acts as a carrier [21].
In this work, the given information which circulates in the optical fiber is represented by the knowledge of the spectral data and the frequency k.
The determination of the function q, in the previous problem (Π''), leads (from (2.1)) to the determination of the exact refractive index n (or at least a numerical approximation of it) which is the objective of this work.

Remark 3.1. In this work, we study the case: $\alpha \in \mathbb{N}^*$.

4 Constraints's Set and Approximation's Functions

Let $m \in \mathbb{N}^*$, such that: $m-1 = \alpha$.

Definition 4.1. We define the feasible set (set of constraints) $\mathcal{C}$ by

$$\mathcal{C} = \left\{ c = (c_0, c_1, ..., c_{m-1})^t \in \mathbb{R}^m / \sum_{j=0}^{m-1} c_j a^j = 0 \right\}. \tag{4.1}$$

Definition 4.2. For each $c = (c_0, c_1, ..., c_{m-1})^t \in \mathcal{C}$, we look for an approximation of $q(r)$ in the form

$$\begin{aligned} p_c(x,y) &= \begin{cases} \sum_{j=0}^{m-1} c_j (\sqrt{x^2+y^2})^j & , 0 \le \sqrt{x^2+y^2} \le a \\ 0 & , \sqrt{x^2+y^2} \ge a \end{cases} \\ &= \begin{cases} \sum_{j=0}^{m-1} c_j r^j & , 0 \le r \le a \\ 0 & , r \ge a \end{cases} \\ &= p_c(r) \end{aligned} \tag{4.2}$$

moreover, we set

$$\mathcal{N}(r) = n^2(r) = n_\infty^2 - \frac{1}{k^2}.q(r) \tag{4.3}$$

$$\mathcal{M}_c(r) = n_\infty^2 - \frac{1}{k^2}.p_c(r) \tag{4.4}$$

for all $r \geq 0$ and for all $c = (c_0, c_1, ..., c_{m-1})^t \in \mathcal{C}$.

The required radial approximation $p_c(r)$ (4.2) is represented (on the interval $[0, a]$) as a finite combination of appropriately chosen basis functions: $1, r, r^2, ..., r^{m-1}$. We determine the coefficients: $c_0, c_1, c_2, ..., c_{m-1}$ (of the combination) by numerical simulations. This is the perspective of the present paper.

Remark 4.3. From (2.1), it follows that q is a continuous and bounded piecewise radially symmetrical polynomial expression.

Remark 4.4. From (4.2), our approximation p_c is also a continuous and bounded piecewise radially symmetrical polynomial expression, for all $c \in \mathcal{C}$.

Corollary 4.5. *By construction, for all $c \in \mathcal{C}$: the function p_c defined in (4.2) is bounded.*

5 Objective of this Work

Our approach would be to solve numerically the inverse eigenvalue problem (Π''), which means the reconstruction of a good approximation of the radial function $q(r)$ (or equivalently (from (4.3)), a good approximation of the radial function $\mathcal{N}(r)$).
So, we want to prove that: $\exists \xi = (\xi_0, \xi_1, ..., \xi_{m-1})^t \in \mathcal{C}$ such that:
$\mathcal{M}_\xi(r)$ ($P_\xi(r)$ respectively) is the best approximation of $\mathcal{N}(r)$ ($q(r)$ respectively) (in $\|.\|_\infty$ norm) (a precise error estimation in the infinity norm).
In other words, our goal is to determine the components $\xi_0, \xi_1, ..., \xi_{m-1}$ of $\xi \in \mathcal{C}$, such that

$$\begin{aligned} \sup_{r\in[0,a]} |\mathcal{M}_\xi(r) - \mathcal{N}(r)| &= \sup_{r\geq 0} |\mathcal{M}_\xi(r) - \mathcal{N}(r)| \\ &= \|\mathcal{M}_\xi(r) - \mathcal{N}(r)\|_\infty \end{aligned} \tag{5.1}$$

is small enough (it tends to 0)

or equivalently

$$\begin{aligned} \sup_{r\in[0,a]} |p_\xi(r) - q(r)| &= \sup_{r\geq 0} |p_\xi(r) - q(r)| \\ &= \|p_\xi(r) - q(r)\|_\infty \end{aligned} \tag{5.2}$$

is small enough (it tends to 0).

6 Useful Main Tools

The following propositions will be useful

Proposition 6.1. *The function ϕ defined by: $\phi : \mathbb{R}^m \longrightarrow \mathbb{R}$, such that*

$$\phi(c) = \sum_{j=0}^{m-1} c_j a^j, \forall c = (c_0, c_1, ..., c_{m-1})^t \in \mathbb{R}^m$$

is obviously an affine function on $\mathbb{R}^m$.

Corollary 6.2. *From (4.1), we obtain that*

$$\mathcal{C} = \Big\{ c = (c_0, c_1, ..., c_{m-1})^t \in \mathbb{R}^m / \ \phi(c) = 0 \Big\}.$$

Proposition 6.3. *$\mathcal{C}$ is a $(non\ empty)$ convex set in the normed space $\mathbb{R}^m$.*

Proof. In fact, the convexity of $\mathcal{C}$ is due to the affinity of the function ϕ.

□

7 Notations and Basic Terminology

Let $R \in \mathbb{R}$ satisfying: $0 < a < R$, and let $l \in \mathbb{N}^*$.
In what follows, for each $c = (c_0, c_1, ..., c_{m-1})^t \in \mathcal{C}$, we denote:
$c^0 = \left(c_0^0, c_1^0, ..., c_{m-1}^0\right)^t \in \mathbb{R}^m$ as an arbitrary starting vector of c,
$\lambda_1(c), \lambda_2(c), ..., \lambda_l(c)$: the l first corresponding eigenvalues (of the direct problem (Π')) to the potential $p_c(r)$,
$\lambda_1, \lambda_2, ..., \lambda_l$: the l first corresponding eigenvalues (of the direct problem (Π')) to the potential $q(r)$,
$\mathbf{\Lambda}(c) = (\lambda_1(c), \lambda_2(c), ..., \lambda_l(c))^t \in \mathbb{R}^l$,
$\mathbf{\Lambda} = (\lambda_1, \lambda_2, ..., \lambda_l)^t \in \mathbb{R}^l$.

The parameters $\xi_0, \xi_1, ..., \xi_{m-1}$ (cited in Section 5) will be evaluated by minimizing the quantity:

$$\|\mathbf{\Lambda} - \mathbf{\Lambda}(c)\|_2^2$$

on the convex set $\mathcal{C}$.
For the sake of this purpose, $\xi = (\xi_0, \xi_1, ..., \xi_{m-1})^t$ will be computed by solving the following optimization problem [8, 13, 22] (7.1) (that will be solved iteratively), posed in the convex set $\mathcal{C}$:

$$c^i = \underset{c \in \mathcal{C}}{argmin} f_i(c), \forall i \in \mathbb{N}^* \tag{7.1}$$

such that: $\forall c \in \mathbb{R}^m, \forall i \in \mathbb{N}^*$:

$$f_i(c) = \|\mathbf{\Lambda} - L_i(c)\|_2^2 \tag{7.2}$$

where $\|.\|_2$ denotes the Euclidean norm, and:

$$L_i(c) = \mathbf{\Lambda}\left(c^{i-1}\right) + \Gamma_i.\left(c - c^{i-1}\right)$$

($\forall i \in \mathbb{N}^*$: $\mathbf{\Lambda}$ is linearized by the linear part $L_i(c)$ of its *Taylor* expansion at c^{i-1})

$$c^{i-1} = \left(c_0^{i-1}, c_1^{i-1}, ..., c_{m-1}^{i-1}\right)^t \in \mathbb{R}^m$$

$$c^i = \left(c_0^i, c_1^i, ..., c_{m-1}^i\right)^t \in \mathbb{R}^m$$

and Γ_i is the real $l \times m$ Jacobian matrix defined by

$$\Gamma_i = \left(\frac{\partial \lambda_p}{\partial c_j}\left(c^{i-1}\right)\right)_{\substack{1 \le p \le l \\ 0 \le j \le m-1}}$$

(Γ_i is called "the linear component of the linearization $L_i(c)$").

In an actual computation, at each step i the components $(c_j^i)_{0 \le j \le m-1}$ of c^i are computed sequentially from the components of c^{i-1} (see (7.1)).
Therefore it is advantageous, in looking at the right side of (7.1), to use those components of c^{i-1} which are already known, instead of the corresponding components of c^i.
In practice, this means that the components of c^i immediately replace those of c^{i-1} in memory. This not only saves memory, but simplifies the program [38].
The previous considerations lead to an algorithm (**Algorithm 8.1** below) that describes a procedure to solve (5.1) and thus (5.2) and therefore handling the resolution of the inverse problem (Π'').

Remark 7.1. Let $1 \le p \le l$, $0 \le j \le m-1$ and $i \in \mathbb{N}^*$.
We note that it is a challenge to apply the following definition

$$\frac{\partial \lambda_p}{\partial c_j}\left(c^{i-1}\right) = \lim_{h \to 0} \frac{\lambda_p(c_0^{i-1}, ..., c_j^{i-1} + h, ..., c_{m-1}^{i-1}) - \lambda_p(c_0^{i-1}, ..., c_j^{i-1}, ..., c_{m-1}^{i-1})}{h}$$

on a computer, because its finite word length causes the numerator to fluctuate between 0 and round-off error as the denominator approaches zero [33].
A simple and effective solution is to make h small but not zero [33]:

$$\frac{\partial \lambda_p}{\partial c_j}\left(c^{i-1}\right) \approx \frac{\delta \lambda_p}{\delta c_j}\left(c^{i-1}\right)$$

therefore

$$\frac{\partial \lambda_p}{\partial c_j}\left(c^{i-1}\right) \approx \frac{\lambda_p\left(c_0^{i-1}, ..., c_j^{i-1}+h, ..., c_{m-1}^{i-1}\right) - \lambda_p\left(c_0^{i-1}, ..., c_j^{i-1}, ..., c_{m-1}^{i-1}\right)}{h} \tag{7.3}$$

(7.3) known as the "forward-difference rule", is not the most accurate approximation, but it will suffice [33].

Proposition 7.2. *For each $i \in \mathbb{N}^*$:*
The cost function f_i defined in (7.2) is a twice differentiable convex function on $\mathbb{R}^m$ (and thus on the convex set $\mathcal{C}$).

Proof. In fact, for each $i \in \mathbb{N}^*$ and for each $c \in \mathbb{R}^m$, we have

$$\begin{aligned} f_i(c) &= \|\Gamma_i c\|_2^2 - 2. < \Gamma_i c, \Lambda - \Lambda(c^{i-1}) + \Gamma_i c^{i-1} > + \left\|\Lambda - \Lambda(c^{i-1}) + \Gamma_i c^{i-1}\right\|_2^2 \\ &= \|\Gamma_i c\|_2^2 - 2.c^t \Gamma_i^t.(\Lambda - \Lambda(c^{i-1}) + \Gamma_i c^{i-1}) + \left\|\Lambda - \Lambda(c^{i-1}) + \Gamma_i c^{i-1}\right\|_2^2 \end{aligned}$$

(where $< .,. >$ denotes the inner product defined on the space $\mathbb{R}^l$)
thus, we can easily show that: $\lim\limits_{h \to 0} \dfrac{f_i(c+h) - f_i(c) - \nabla f_i(c).h}{\|h\|_2} = 0$, where

$$\begin{aligned} \nabla f_i(c) &= 2.\Gamma_i^t.\Gamma_i.c - 2.\Gamma_i^t.(\Lambda - \Lambda(c^{i-1}) + \Gamma_i c^{i-1}) \\ &= 2.\Gamma_i^t.(\Gamma_i.c - \Gamma_i.c^{i-1} + \Lambda(c^{i-1}) - \Lambda). \end{aligned}$$

Since $\nabla f_i : \mathbb{R}^m \longrightarrow \mathbb{R}^m$ is an affine function, then, it is differentiable [24, 32, 59] on $\mathbb{R}^m$ and we have

$$\nabla^2 f_i(c) = 2.\Gamma_i^t.\Gamma_i, \forall c \in \mathbb{R}^m.$$

Otherwise: $\forall c \in \mathbb{R}^m, \forall c^{'} \in \mathbb{R}^m, \forall \eta \in [0,1]$, we have

$$\begin{aligned} f_i(\eta.c + (1-\eta).c^{'}) &= \left\|\Lambda - L_i(\eta.c + (1-\eta).c^{'})\right\|_2^2 \\ &= \left\|\Lambda - \Lambda(c^{i-1}) - \Gamma_i(\eta.c + (1-\eta).c^{'} - c^{i-1})\right\|_2^2 \\ &= \left\|(\eta + (1-\eta)).(\Lambda - \Lambda(c^{i-1})) - \eta.\Gamma_i.c - (1-\eta).\Gamma_i.c^{'} + (\eta + (1-\eta)).\Gamma_i.c^{i-1}\right\|_2^2 \\ &= \left\|\eta.(\Lambda - \Lambda(c^{i-1}) + \Gamma_i.c^{i-1} - \Gamma_i.c) + (1-\eta).(\Lambda - \Lambda(c^{i-1}) + \Gamma_i.c^{i-1} - \Gamma_i.c^{'})\right\|_2^2 \\ &= \left\|\eta.(\Lambda - L_i(c)) + (1-\eta).(\Lambda - L_i(c^{'}))\right\|_2^2 \end{aligned}$$

but, since the function $g : \mathbb{R}^m \longrightarrow \mathbb{R}_+$ defined by

$$g(x) = \|x\|_2^2, \forall x \in \mathbb{R}^m$$

is convex (it is even strongly convex [2, 34, 44]) on $\mathbb{R}^m$, it follows

$$\begin{aligned} f_i(\eta.c + (1-\eta).c^{'}) &\leq \eta.\left\|\Lambda - L_i(c)\right\|_2^2 + (1-\eta).\left\|\Lambda - L_i(c^{'})\right\|_2^2 \\ &= \eta.f_i(c) + (1-\eta).f_i(c^{'}) \end{aligned}$$

hence, the function f_i is convex on $\mathbb{R}^m$ and consequently on $\mathcal{C}$. □

From **Proposition 7.2.**, we deduce that (7.1) is a constrained convex optimization problem. Otherwise, the following well known Theorem (which will be useful for the present work) summarizes necessary and sufficient conditions for convex optimization

Theorem 7.3. ([47], page 57)
Let $\mathcal{U}$ be an open convex set. If f is a differentiable convex function on $\mathcal{U}$, $\phi_1, \phi_2, ..., \phi_p$ $(p \in \mathbb{N}^*)$ are affine functions on $\mathcal{U}$, and

$$\mathcal{D} = \left\{ c \in \mathcal{U} : \phi_i(c) = 0, \forall i = 1, 2, ..., p \right\}$$

then:

(c^* is a global minimum of f on $\mathcal{D}$) $\Longleftrightarrow \exists (\mu_i)_{1 \leq i \leq p} \nabla f(c^*) + \sum_{i=1}^{p} \mu_i \nabla \phi_i(c^*) = 0.$

$\mu_1, \mu_2, ..., \mu_p \in \mathbb{R}$ are called "Lagrange multipliers" [8, 17, 56, 58, 60].

The method of *Lagrange* multipliers is the usual elegant approach taught in multivariable calculus courses for locating the extrema of a function of several variables subject to one or more constraints [41].

8 The Algorithm of Adopted Method

In this section, we will describe an optimization-based algorithm for solving the inverse problem previously considered. Here is the description of our method's generic Algorithm

Algorithm 8.1

Let α, m and l be fixed numbers (previously defined in Section 1, Section 4 and Section 7 (respectively)).
Choose $\epsilon > 0$ (a tolerance error) small enough (this will ensure the convergence of our Algorithm).
Pick an arbitrary starting vector $c^0 \in \mathbb{R}^m$ of $c \in \mathcal{C}$, where $c^0 = \left(c_0^0, c_1^0, ..., c_{m-1}^0\right)^t$ and
$c = (c_0, c_1, ..., c_{m-1})^t$.

The beginning of the Algorithm. Iterate until convergence

- **Step 1**: $i = 1$: **(Initialization)**.

  Applying **Theorem 7.3.** and **Proposition 7.2.**, we conclude that

  $$c^1 = \underset{c \in \mathcal{C}}{argmin} f_1(c) \Longleftrightarrow \exists \mu^1 \in \mathbb{R} : \nabla f_1(c^1) + \mu^1 \nabla \phi(c^1) = 0.$$

  - Compute μ^1 and the components of c^1.

- **Step** *i*: $i \geq 2$.

  From **Theorem 7.3.** and **Proposition 7.2.**, it follows

  $$c^i = \underset{c \in \mathcal{C}}{argmin} f_i(c) \Longleftrightarrow \exists \mu^i \in \mathbb{R} : \nabla f_i(c^i) + \mu^i \nabla \phi(c^i) = 0.$$

  - Compute μ^i and the components of c^i.
  - While: $\|\mathcal{M}_{c^i} - \mathcal{N}\|_\infty > \epsilon$, do: update: $i \longleftarrow i + 1$.

- **Last Step**: **(The stopping criterion)**
Repeat the last minimization process (step *i*), until we get:
$\exists i_0 \geq 2 : c^{i_0} \in \mathcal{C}$ such that

$$\|\mathcal{M}_{c^{i_0}} - \mathcal{N}\|_\infty = \frac{1}{k^2}. \|p_{c^{i_0}} - q\|_\infty \leq \epsilon \text{ (henceforth, we set: } \xi = c^{i_0})$$

(the convergence is satisfied).

Stop (The end of the Algorithm).

Remark 8.1. In the previous Algorithm, we note that at each step i $(1 \leq i \leq i_0)$: $\mu^i \neq 0$ and μ^i can have either sign (as we will see in the next section (Numerical results and discussion)).

8.1 Properties of Algorithm 8.1

It is striking to remark that **Algorithm 8.1** satisfies some basic properties

- No calculation of second derivatives is required, only the gradient of the cost function defined in (7.2) and the gradient of the function ϕ defined in **Proposition 6.1.** are calculated at each iteration.
- Only one vector (μ_i and the components of c^i) to be stored at each iteration $i \in \mathbb{N}^*$, contrary to other methods (that need, for example, to store all the elements of the Hessian matrix).
- **Algorithm 8.1** is attractive for its very cheap computational cost.
- Numerical errors which are generated during the solution of discretized equations are small.
- Correctness and convergence: The numerical solution tends to the exact solution from one step to the next one.
- Finiteness and effectiveness: This algorithm always finishes after a few steps (small number of steps).

Remark 8.2. The properties mentioned above will be justified in the next section (Numerical results and discussion).

Remark 8.3. At each step $i \geq 1$ in **Algorithm 8.1** (which is of order 1, since it uses the gradient of the cost function), the use of **Theorem 7.3.** amounts to solving the following non-homogeneous linear system $(\Pi^i_{l,m})$ of $(m+1)$ equations in $(m+1)$ unknowns $(reals)$: $c^i_0, c^i_1, ..., c^i_{m-1}$ and μ^i:

$$(\Pi^i_{l,m})\begin{cases} 2.\displaystyle\sum_{p=1}^{l}\left(\lambda_p-\lambda_p\left(c^{i-1}\right)-\sum_{j=0}^{m-1}\frac{\partial\lambda_p}{\partial c_j}(c^{i-1}).(c^i_j-c^{i-1}_j)\right).\left(-\frac{\partial\lambda_p}{\partial c_0}(c^{i-1})\right)+\mu^i=0 \;....\;(1^{st}\;equation)\\ 2.\displaystyle\sum_{p=1}^{l}\left(\lambda_p-\lambda_p\left(c^{i-1}\right)-\sum_{j=0}^{m-1}\frac{\partial\lambda_p}{\partial c_j}(c^{i-1}).(c^i_j-c^{i-1}_j)\right).\left(-\frac{\partial\lambda_p}{\partial c_1}(c^{i-1})\right)+\mu^i a=0 \;....\;(2^{nd}\;equation)\\ \dots\dots\dots\dots\dots\dots\dots\dots\\ \dots\dots\dots\dots\dots\dots\dots\dots\\ \dots\dots\dots\dots\dots\dots\dots\dots\\ 2.\displaystyle\sum_{p=1}^{l}\left(\lambda_p-\lambda_p\left(c^{i-1}\right)-\sum_{j=0}^{m-1}\frac{\partial\lambda_p}{\partial c_j}(c^{i-1}).(c^i_j-c^{i-1}_j)\right).\left(-\frac{\partial\lambda_p}{\partial c_{m-1}}(c^{i-1})\right)+\mu^i a^{m-1}=0 \;....\;(m^{th}\;equation)\\ c^i_0+ac^i_1+a^2c^i_2+...+a^{m-1}c^i_{m-1}=0 \;....\;((m+1)^{th}\;equation) \end{cases}$$

For better understanding, it was found that for each iteration $i \geq 1$, the matrix A_i associated to the linear system $(\Pi^i_{l,m})$ is invertible (since we can rewrite $(\Pi^i_{l,m})$ in the form: $A_i.x_i = b_i$, where x_i=$(c^i_0, c^i_1, ..., c^i_{m-1}, \mu^i)^t$), thus proving the existence and the uniqueness of the minimum of the cost function f_i. Fortunately, the system $(\Pi^i_{l,m})$ is often easy to solve. Its resolution is done using MAPLE [9, 19, 27, 45].

9 Numerical Results and Discussion

In order to construct a best approximation of the exact refraction index $n(r)$, we used **Algorithm 8.1**. Three realized numerical tests have been made by considering the problem (Π') with the homogeneous Dirichlet condition (for: $\gamma_2 = 0$ and $g = 0$).
In Figures:

Figure 5 and Figure 6 (1^{st} example),
Figure 9 and Figure 10 (2^{nd} example),
Figure 15 and Figure 16 (3^{rd} example),
we plot the curves of the true functions $\mathcal{N}(r)$ and $q(r)$, and their approximations $\mathcal{M}_\xi(r)$ and $p_\xi(r)$ (respectively) in terms of r, and in Figures:
Figure 7 and Figure 8 (1^{st} example),
Figure 11, Figure 12, Figure 13 and Figure 14 (2^{nd} example),
Figure 17 and Figure 18 (3^{rd} example),
we present the variations of $\left|\lambda_p - \lambda_p(c^i)\right|$, $(1 \leq p \leq l)$ in terms of the number of iterations i. We also note that in Table 1, Table 2 and Table 3, the difference $\left|\lambda_p - \lambda_p(c^i)\right|$ converges to 0 when c^i converges to ξ. This proves that the approximate eigenvalues $\lambda_p(c^i)$ converge to the exact eigenvalues λ_p when c^i converges to ξ.
In Figures: Figure 19, Figure 20 and Figure 21, we plot (for $\alpha = 1$, $\alpha = 2$ and $\alpha = 3$ respectively) the curves representing the true function q and its approximation p_ξ, and this in cartesian coordinates, so: $z = q(x, y)$ and $z = p_\xi(x, y)$ where: $0 \leq r = \sqrt{x^2 + y^2} \leq a$.
(We note that: $q(x, y) = p_\xi(x, y) = 0, \forall (x, y) \in \mathbb{R}^2$: $r = \sqrt{x^2 + y^2} \geq a$).
In these Figures: The Blue surface represents the true function q whereas its approximation function p_ξ is represented in red (lines), the three Figures demonstrate the potential of our adopted technique, since we see that the curves of q and p_ξ are almost identical in the three examples (cited in this section).
All the curves, presented in what follows, prove a good accuracy (of the numerical adopted method in this work), and the rapid convergence of our results to the exact solution. In fact, we found that the function $\mathcal{M}_\xi$ represents a good approximation of the function $\mathcal{N} = n^2$, which is none other than the square of the exact refractive index n. Otherwise, the numerical method adopted in our work converges geometrically since:

$$\exists s \in]0, 1[\,, \exists \beta > 0, \exists j_0 \in \mathbb{N} : \left\|\mathcal{M}_{c^j} - \mathcal{N}\right\|_\infty \leq \beta . s^j \tag{9.1}$$

at each iteration $j \geq j_0$.

9.1 First example: A linear index profile ($\alpha = 1$)

Required data for Algorithm 8.1: $m - 1 = 1$, $l = 2$, $\epsilon = 3 \times 10^{-7}$.

Opto-geometrical data:
$V = 3, k = 18.7602, n_+ = 1.5085, n_\infty = 1.5, a = 1, R = a + 20.h, h = 0.04$.

Here, in (9.1) we found that: $\beta = 10^{-1}, s = 0.10013$ and $j_0 = 0$.

For each $i : 0 \leq i \leq 4$, we have: $\Delta_1^i = \left|\lambda_1 - \lambda_1(c^i)\right|$ and $\Delta_2^i = \left|\lambda_2 - \lambda_2(c^i)\right|$.
In this example, we took:

$$q(r) = \begin{cases} -9 + 9r & , 0 \leq r \leq a \\ 0 & , a \leq r \leq R \end{cases}$$

$$\forall c = (c_0, c_1)^t \in \mathcal{C} : \quad p_c(r) = \begin{cases} c_0 + c_1 r & , 0 \leq r \leq a \\ 0 & , a \leq r \leq R \end{cases}$$

We deduce from (4.3) and (4.4) that:
$n^2(r) = \mathcal{N}(r) = 2.25 - 0.00284.q(r)$ and $\mathcal{M}_c(r) = 2.25 - 0.00284.p_c(r)$.
After five iterations, we have reached the following result:
$\|p_\xi - q\|_\infty = 0,0001$, $\|\mathcal{M}_\xi - \mathcal{N}\|_\infty = 2.8414 \times 10^{-7}$, $\Delta_1^4 = \Delta_2^4 = 0.00000$,
for $\xi = (-8.9999, 8.9999)^t = c^4$, and then:

$$p_\xi(r) = \begin{cases} -8.9999 + 8.9999r & , 0 \leq r \leq a \\ 0 & , a \leq r \leq R \end{cases}$$

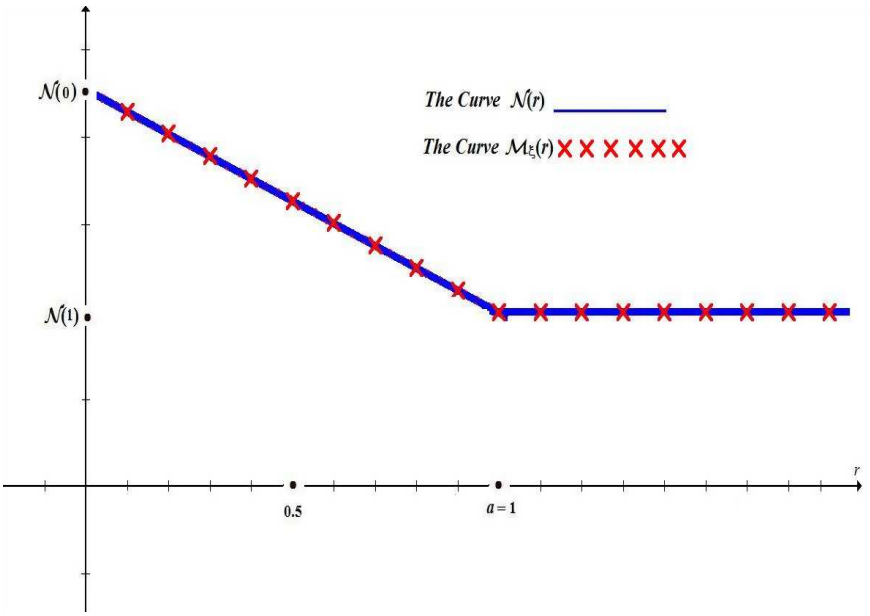

Figure 5: The curves of $\mathcal{N}(r)$ and $\mathcal{M}_\xi(r)$ for $\xi = c^4$ & $\alpha = 1$

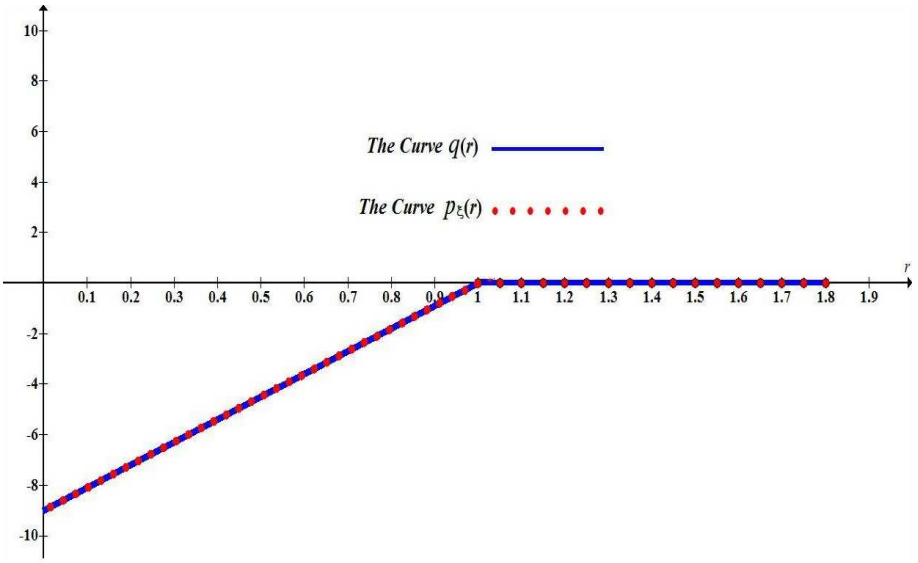

Figure 6: The curves of $q(r)$ and $p_\xi(r)$ for $\xi = c^4$ & $\alpha = 1$

We summarize the achieved results during the five iterations within Table 1 (where we see that the accuracy (in the seventh column) is $O(10^{-7})$ for $\alpha = 1$):

Table 1: The running of **Algorithm 8.1** for $\alpha = 1$

Iteration	**Solution**		**Magnitude of the errors**			
i	c_0^i	c_1^i	Δ_1^i	Δ_2^i	$\|p_{c^i} - q\|_\infty$	$\|\mathcal{M}_{c^i} - \mathcal{N}\|_\infty$
0	1.	0.	4.07298	1.85147	10	2.8414×10^{-2}
1	-12.524	12.524	1.67031	0.7032	3.524	1.0013×10^{-2}
2	-9.175	9.175	0.07894	0.03259	0.175	4.9724×10^{-4}
3	-9.0006	9.0006	0.00031	0.00013	0.0006	1.7048×10^{-6}
4	-8.9999	8.9999	0.00000	0.00000	0.0001	2.8414×10^{-7}

	***Lagrange* multiplier**	**Cost function at c^i**
i	μ^i	$f_i(c^i)$
0	/	/
1	7.2637×10^{-3}	3.670333
2	-7.0776×10^{-3}	4.964810
3	7.4367×10^{-5}	4.407511
4	9.1648×10^{-7}	4.370587

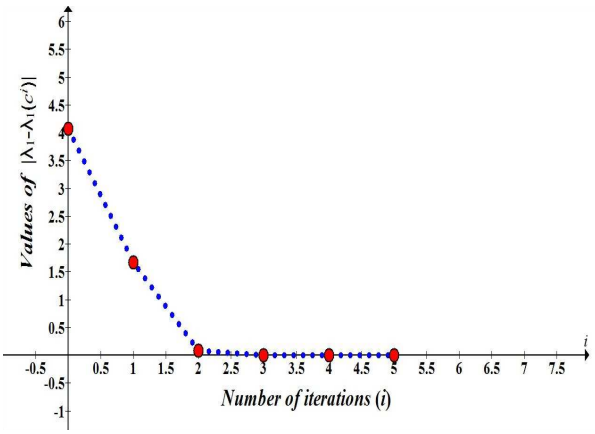

Figure 7: Variation of $\left|\lambda_1 - \lambda_1(c^i)\right|$ in terms of number of iterations i

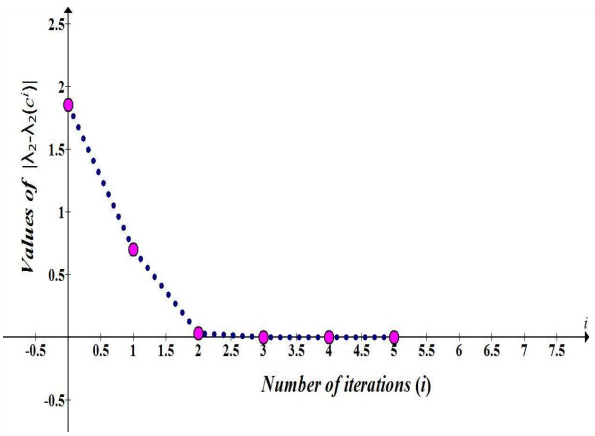

Figure 8: Variation of $\left|\lambda_2 - \lambda_2(c^i)\right|$ in terms of number of iterations i

9.2 Second example: A parabolic index profile ($\alpha = 2$)

Required data for Algorithm 8.1: $m - 1 = 2$, $l = 4$, $\epsilon = 1.5 \times 10^{-6}$.

Opto-geometrical data:
$V = 4, k = 25.01356, n_+ = 1.5085, n_\infty = 1.5, a = 1, R = a + 20.h, h = 0.04.$

Here, in (9.1), we found that: $\beta = 10^{-1}, s = 0.27171$ and $j_0 = 4$.

For each $i : 0 \leq i \leq 8$, we have:
$\Delta_1^i = \left|\lambda_1 - \lambda_1(c^i)\right|, \Delta_2^i = \left|\lambda_2 - \lambda_2(c^i)\right|, \Delta_3^i = \left|\lambda_3 - \lambda_3(c^i)\right|, \Delta_4^i = \left|\lambda_4 - \lambda_4(c^i)\right|.$
In this example, we took:

$$q(r) = \begin{cases} -16 + 16r^2 & , 0 \leq r \leq a \\ 0 & , a \leq r \leq R \end{cases}$$

$$\forall c = (c_0, c_1, c_2)^t \in \mathcal{C} : \quad p_c(r) = \begin{cases} c_0 + c_1 r + c_2 r^2 & , 0 \leq r \leq a \\ 0 & , a \leq r \leq R \end{cases}$$

We deduce from (4.3) and (4.4) that:

$$n^2(r) = \mathcal{N}(r) = 2.25 - 0.001598.q(r) \quad \text{and} \quad \mathcal{M}_c(r) = 2.25 - 0.001598.p_c(r).$$

After nine iterations, we have reached the following result:
$\|p_\xi - q\|_\infty = 7.7222 \times 10^{-4}$, $\|\mathcal{M}_\xi - \mathcal{N}\|_\infty = 1.2342 \times 10^{-6}$,
$\Delta_1^8 = 0.00000, \Delta_2^8 = 0.000177, \Delta_3^8 = 0.00001, \Delta_4^8 = 0.00027$,
for $\xi = (-16.002, 0.0081568, 15.994)^t = c^8$, and then:

$$p_\xi(r) = \begin{cases} -16.002 + 0.0081568r + 15.994r^2 & , 0 \leq r \leq a \\ 0 & , a \leq r \leq R \end{cases}$$

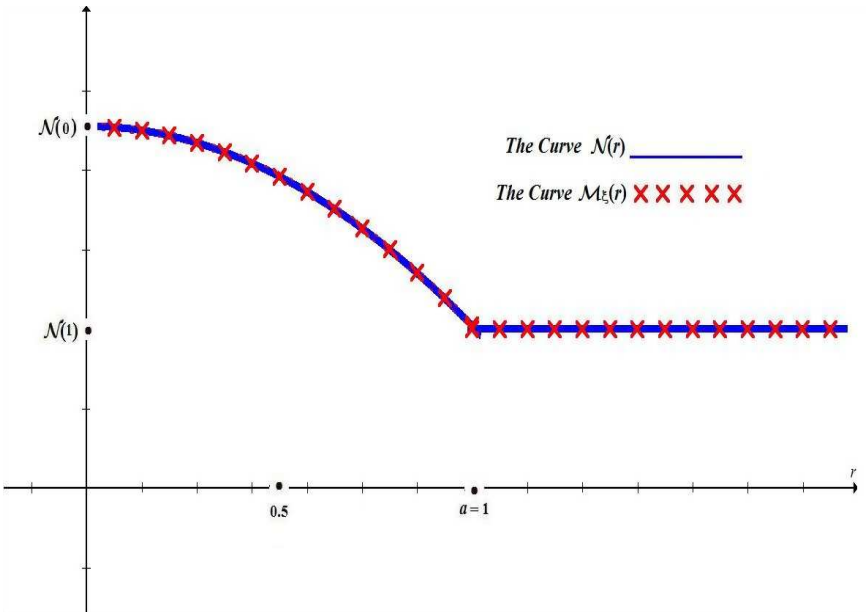

Figure 9: The curves of $\mathcal{N}(r)$ and $\mathcal{M}_\xi(r)$ for $\xi = c^8$ & $\alpha = 2$

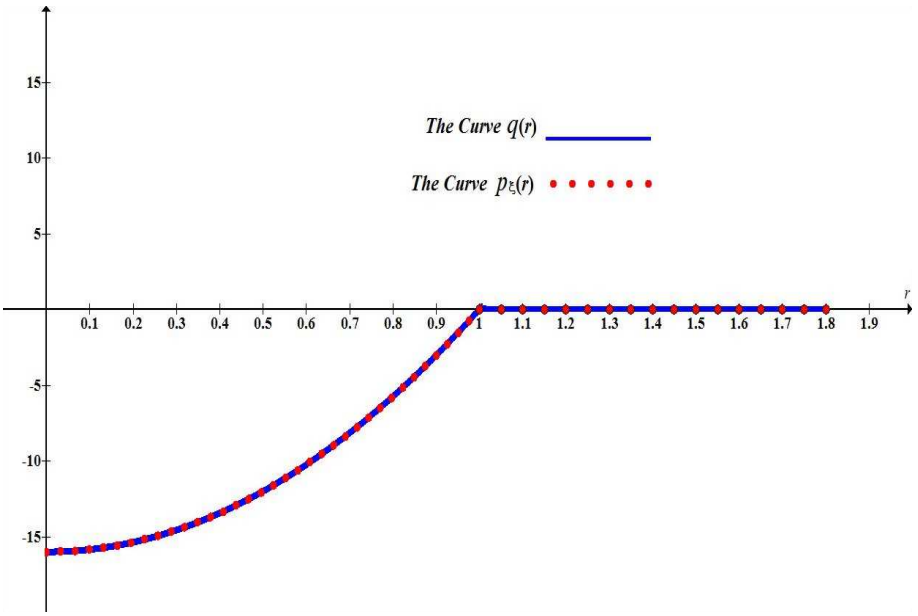

Figure 10: The curves of $q(r)$ and $p_\xi(r)$ for $\xi = c^8$ & $\alpha = 2$

We summarize the achieved results during the nine iterations within Table 2 (where we see that the accuracy (in the eleventh column) is $O(10^{-6})$ for $\alpha = 2$):

Table 2: The running of **Algorithm 8.1** for $\alpha = 2$

Iteration	**Solution**		
i	c_0^i	c_1^i	c_2^i
0	1.	0.	0.
1	26.766	-157.15	130.38
2	-1.5098	-51.149	52.659
3	-9.508	-22.411	31.919
4	-16.451	1.1768	15.274
5	-16.003	0.01092	15.992
6	-16.002	0.008114	15.994
7	-16.002	0.008208	15.994
8	-16.002	0.0081568	15.994

Remaining of Table 2

Magnitude of the errors

i	Δ_1^i	Δ_2^i	Δ_3^i	Δ_4^i	$\|p_{c^i} - q\|_\infty$	$\|\mathcal{M}_{c^i} - \mathcal{N}\|_\infty$
0	10.58557	5.69479	13.40442	15.65374	17	2.7171×10^{-2}
1	18.84316	7.43456	5.434838	11.90609	11.212	1.792×10^{-2}
2	0.27665	1.5431	0.50241	0.21555	3.3516	5.3567×10^{-3}
3	0.35756	0.59013	0.27649	0.51484	1.3956	2.2305×10^{-3}
4	0.10751	0.021264	0.03999	0.00209	2.588×10^{-2}	4.1363×10^{-5}
5	0.00026	0.000282	0.00014	0.00022	7.2645×10^{-4}	1.1611×10^{-6}
6	0.00002	0.000199	0.00002	0.00025	7.4321×10^{-4}	1.1878×10^{-6}
7	0.00002	0.000151	0.00000	0.00029	8.0714×10^{-4}	1.29×10^{-6}
8	0.00000	0.000177	0.00001	0.00027	7.7222×10^{-4}	1.2342×10^{-6}

	***Lagrange* multiplier**	**Cost function at c^i**
i	μ^i	$f_i(c^i)$
0	/	/
1	1.1603×10^{-1}	14.48687×10^{-1}
2	1.6458×10^{-1}	16.15612×10^{-1}
3	1.0011×10^{-1}	9.848410×10^{-1}
4	1.2859×10^{-2}	6.393739×10^{-2}
5	1.4066×10^{-4}	7.856362×10^{-4}
6	-3.6208×10^{-5}	3.2723×10^{-4}
7	-3.708×10^{-5}	3.244157×10^{-4}
8	-3.6781×10^{-5}	3.232053×10^{-4}

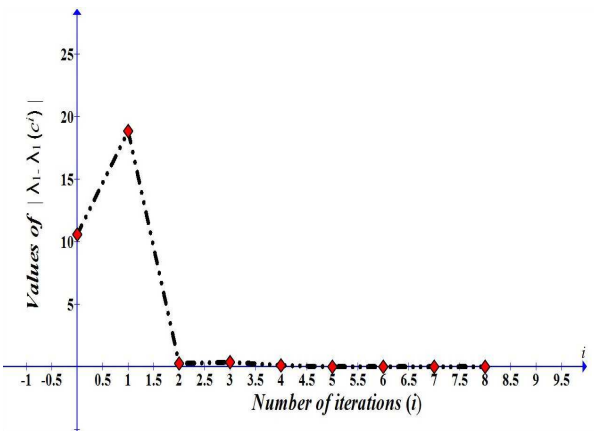

Figure 11: Variation of $\left|\lambda_1 - \lambda_1(c^i)\right|$ in terms of number of iterations i

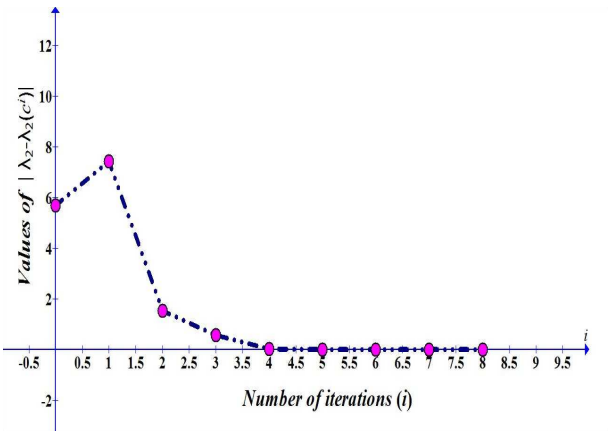

Figure 12: Variation of $\left|\lambda_2 - \lambda_2(c^i)\right|$ in terms of number of iterations i

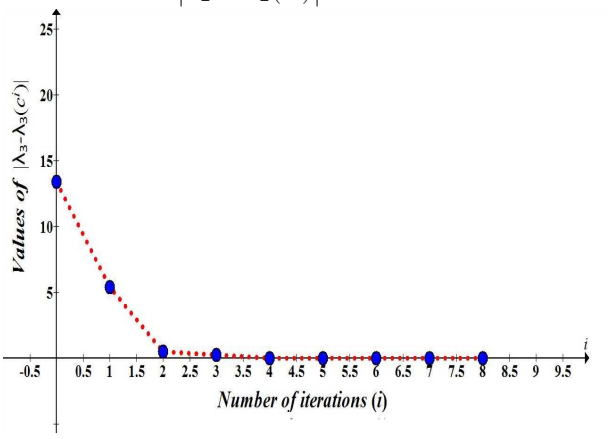

Figure 13: Variation of $\left|\lambda_3 - \lambda_3(c^i)\right|$ in terms of number of iterations i

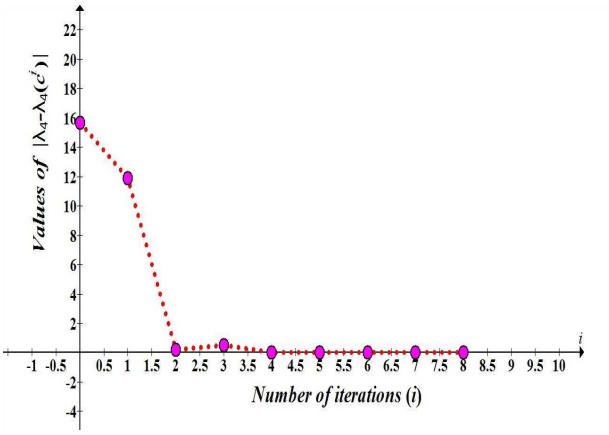

Figure 14: Variation of $\left|\lambda_4 - \lambda_4(c^i)\right|$ in terms of number of iterations i

9.3 Third example: A cubic index profile ($\alpha = 3$)

Required data for Algorithm 8.1: $m - 1 = 3$, $l = 2$, $\epsilon = 4.5 \times 10^{-5}$.

Opto-geometrical data:
$V = 3, k = 18.7602, n_+ = 1.5085, n_\infty = 1.5, a = 1, R = a + 20.h, h = 0.04.$

Here, in (9.1) we found that: $\beta = 10^{-1}, s = 0.28414$ and $j_0 = 3$.

For each $i : 0 \leq i \leq 5$, we have: $\Delta_1^i = \left|\lambda_1 - \lambda_1(c^i)\right|, \Delta_2^i = \left|\lambda_2 - \lambda_2(c^i)\right|$.
In this example, we took:

$$q(r) = \begin{cases} -9 + 9r^3 & , 0 \leq r \leq a \\ 0 & , a \leq r \leq R \end{cases}$$

$$\forall c = (c_0, c_1, c_2, c_3)^t \in \mathcal{C} : \quad p_c(r) = \begin{cases} c_0 + c_1 r + c_2 r^2 + c_3 r^3 & , 0 \leq r \leq a \\ 0 & , a \leq r \leq R \end{cases}$$

We deduce from (4.3) and (4.4) that:

$$n^2(r) = \mathcal{N}(r) = 2.25 - 0.00284.q(r) \quad \text{and} \quad \mathcal{M}_c(r) = 2.25 - 0.00284.p_c(r).$$

After six iterations, we have reached the following result:
$\|p_\xi - q\|_\infty = 0.015572$, $\|\mathcal{M}_\xi - \mathcal{N}\|_\infty = 4.4246 \times 10^{-5}$,
$\Delta_1^5 = 0.00000$, $\Delta_2^5 = 0.00000$,
for $\xi = (-9.0514, 0.23249, -0.23249, 9.0514)^t = c^5$, and then:

$$p_\xi(r) = \begin{cases} -9.0515 + 0.23249r - 0.23249r^2 + 9.0515r^3 & , 0 \leq r \leq a \\ 0 & , a \leq r \leq R \end{cases}$$

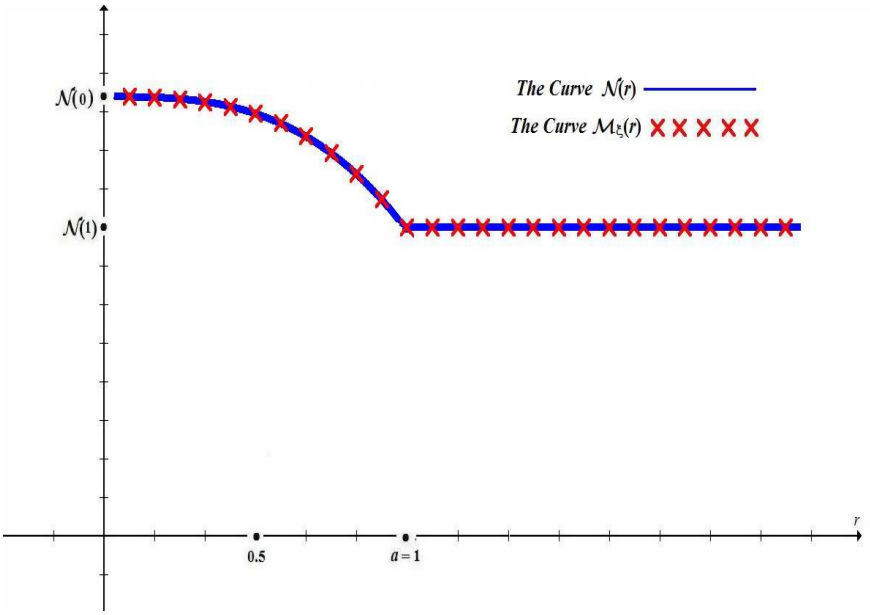

Figure 15: The curves of $\mathcal{N}(r)$ and $\mathcal{M}_\xi(r)$ for $\xi = c^5$ & $\alpha = 3$

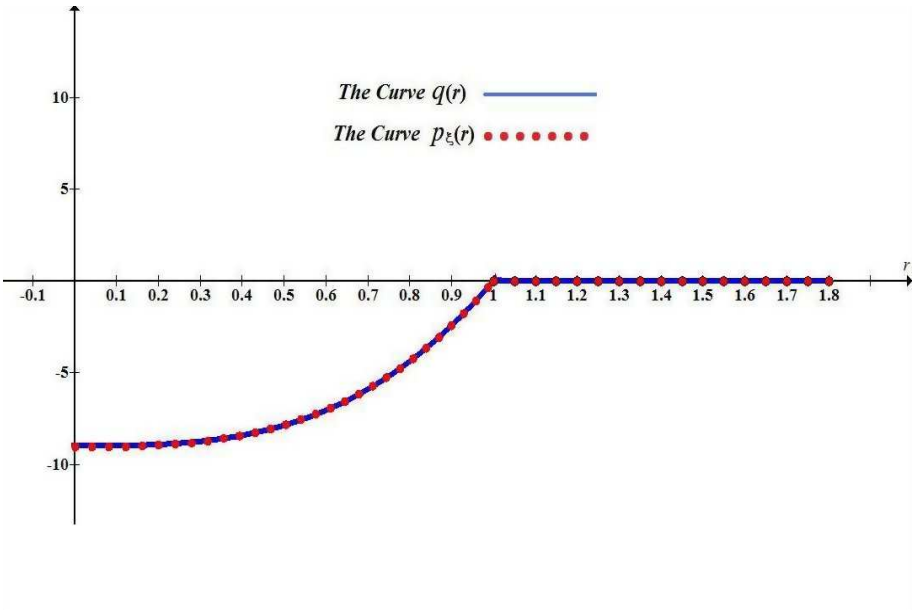

Figure 16: The curves of $q(r)$ and $p_\xi(r)$ for $\xi = c^5$ & $\alpha = 3$

We summarize the achieved results during the six iterations within Table 3 (where we see that the accuracy (in the tenth column) is $O(10^{-5})$ for $\alpha = 3$):

Table 3: The running of **Algorithm 8.1** for $\alpha = 3$

Iteration	**Solution**			
i	c_0^i	c_1^i	c_2^i	c_3^i
0	1.	0.	0.	0.
1	-5.4627	-25.902	25.902	5.4627
2	-8.1109	-3.8288	3.8288	8.1109
3	-9.0693	0.29702	-0.29702	9.0693
4	-9.0522	0.23516	-0.23516	9.0522
5	-9.0515	0.23249	-0.23249	9.0515

	Magnitude of the errors			
i	Δ_1^i	Δ_2^i	$\|p_{c^i} - q\|_\infty$	$\|\mathcal{M}_{c^i} - \mathcal{N}\|_\infty$
0	6.47533	3.60217	10	2.8414×10^{-2}
1	2.17024	1.962653	89.852	2.553×10^{-2}
2	0.04486	0.11331	2.9397	8.3527×10^{-3}
3	0.00144	0.00052	0.017306	4.9173×10^{-5}
4	0.00003	0.00004	0.01567	4.4524×10^{-5}
5	0.00000	0.00000	0.015572	4.4246×10^{-5}

Remaining of Table 3

	***Lagrange* multiplier**	**Cost function at c^i**
i	μ^i	$f_i(c^i)$
0	/	/
1	4.8×10^{-8}	4.599891×10^{-5}
2	4.885×10^{-8}	2.095131×10^{-5}
3	-7.4582×10^{-8}	3.247850×10^{-5}
4	-1.9042×10^{-8}	4.232537×10^{-6}
5	-4.5234×10^{-8}	9.852650×10^{-7}

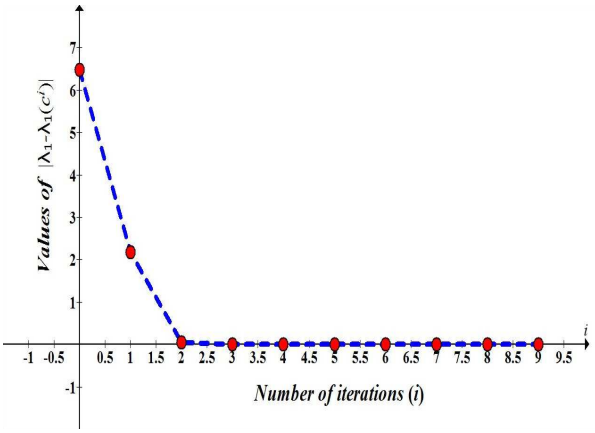

Figure 17: Variation of $\left|\lambda_1 - \lambda_1(c^i)\right|$ in terms of number of iterations i

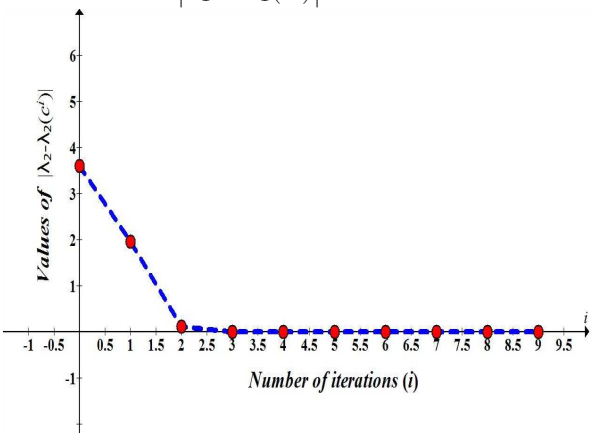

Figure 18: Variation of $\left|\lambda_2 - \lambda_2(c^i)\right|$ in terms of number of iterations i

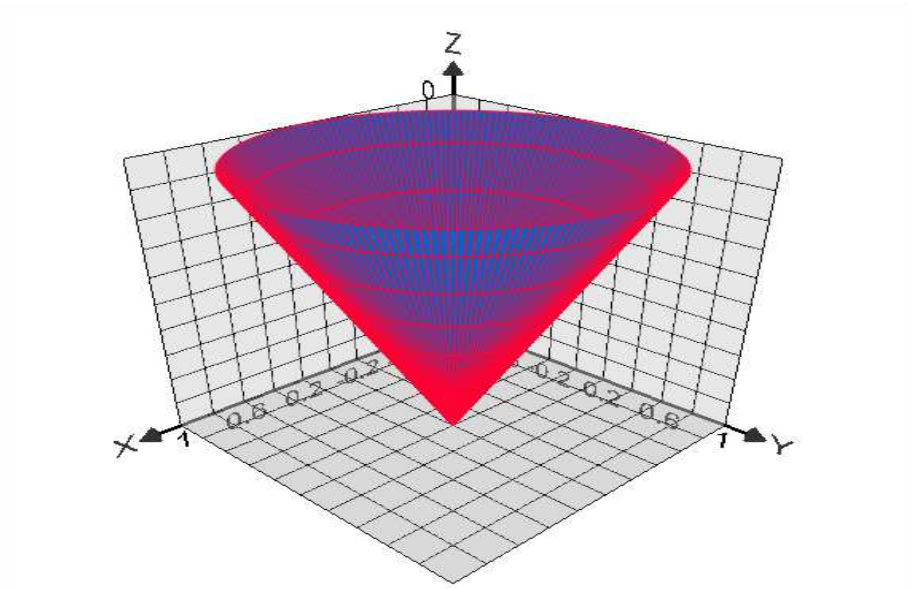

Figure 19: The curves: $z = q(x, y)$ & $z = p_\xi(x, y)$ (where: $\sqrt{x^2 + y^2} \leq a$) for $\xi = c^4$ & $\alpha = 1$ (First example)

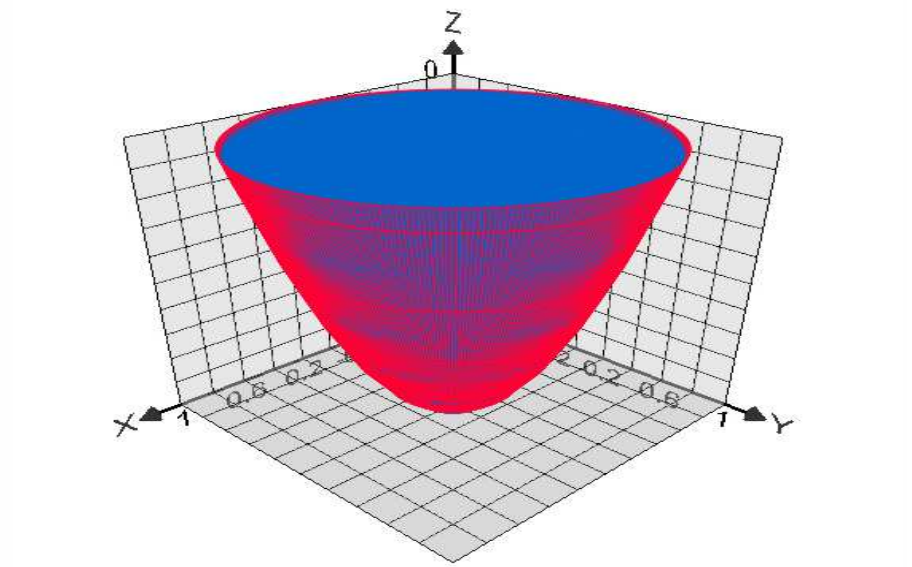

Figure 20: The curves: $z = q(x, y)$ & $z = p_\xi(x, y)$ (where: $\sqrt{x^2 + y^2} \leq a$) for $\xi = c^8$ & $\alpha = 2$ (Second example)

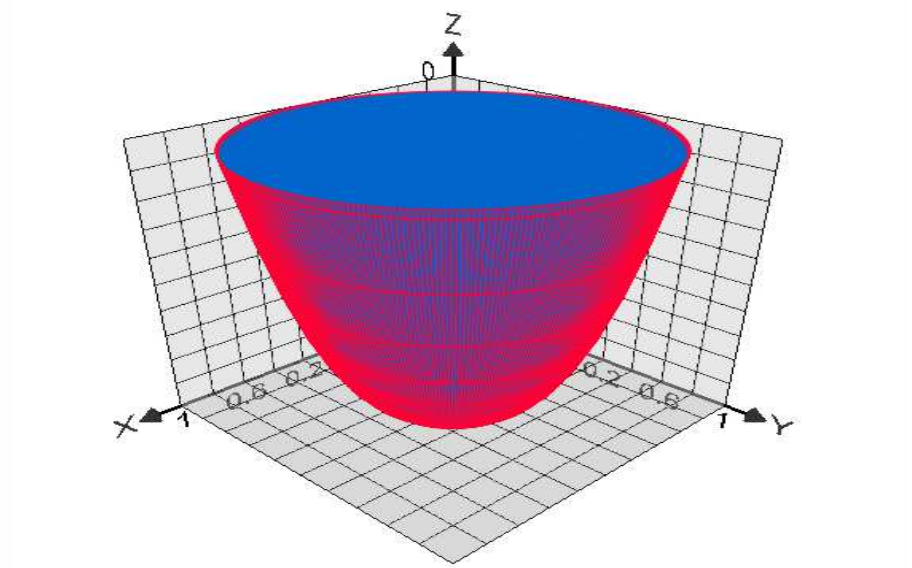

Figure 21: The curves: $z = q(x, y)$ & $z = p_\xi(x, y)$ (where: $\sqrt{x^2 + y^2} \leq a$) for $\xi = c^5$ & $\alpha = 3$ (Third example)

10 Conclusion

In conclusion, this paper deals with a special inverse eigenvalue problem solved by a finite Algorithm.
In fact, in this work, we aimed to the development of a numerical method (easy to implement) in order to solve an inverse eigenvalue problem of computing guided modes in graded-index optical fibers (direct problem). This last was solved by a finite element method.
The numerical reconstruction of the exact refractive-index was one of our ultimate goals in this paper.
We have proposed a fast algorithm to accomplish this objective, then we have synthesized obtained numerical results using *Lagrange* multipliers and a constrained convex optimization (minimization) method to solve the inverse eigenvalue problem mentioned above.
Numerical results obtained in this work, show that the reconstructed refractive-index agrees with the true refractive-index (with relatively high accuracy), proving the effectiveness, computational efficiency and good accuracy of our approach.
During the numerical resolution of each linear system (obtained from the minimization process), it was found that its associated matrix is invertible proving the existence and the uniqueness of this minimum.
In the other hand, it was also found, that the obtained extremum is a global minimum (since all the used domains and functions are convex). Thus, proving the existence and the uniqueness of the sought refractive-index.
We note here that any information on specific values of eigenfunctions (of the direct problem) was not required.
The interest of the work realized in this paper is to determine a perfect approximation of the exact refractive-index profile of an optical fiber having a circular cross section, and this knowing only the frequency and a finite number of spectral data (associated to the direct problem).

11 Future Works and Perspectives

The numerical method (that converges geometrically) proposed in this paper has been successfully introduced for estimating the exact refractive-index, and it can be extended in the same way to more similar or general cases:

- It can be extended to optical fibers of any refractive-index (not necessarily graded-index as we have seen in this paper).
- It can be extended to arbitrarily shaped optical fibers (the cross section may not be necessarily circular, it may be triangular, square, rectangular or even arbitrary).
- It can be extended too to optical fibers of graded-index profile, but for any power parameter α (α may not be an integer as it was taken in this work).
- The same numerical method adopted in this article can be proposed to solve other more complicated mathematical or physical problems.

Strictly speaking, much more hard and productive work is required, and is expected to further our assessment and understanding of the promising obtained results and skills outlined in this paper, which will be needed across future works.

Acknowledgments

The authors would like to express their heartfelt gratitude to Professor A. Badawi, Professor S. Khoury and the anonymous reviewer for their helpful remarks, insightful suggestions, constructive corrections and encouraging comments which helped them to improve their manuscript.

References

[1] T. V. Andersen, *Applications of Nonlinear Optics and Optical Fibers*, Ph.D. Thesis, University of Aarhus, Denmark, 2006.

[2] H. Angulo, J. Giménez, A. M. Moros and K. Nikodem, On Strongly h-Convex Functions, *Ann. Funct. Anal.*, **2(2)**, 85–91 (2011).

[3] Z. J. Bai, *Numerical Methods for Inverse Eigenvalue Problems*, Ph.D. Thesis, The Chinese University of Hong Kong, Hong Kong, 2004.

[4] G. Bal, *Introduction to Inverse Problems*, Columbia University, New York, 2012.

[5] L. Beilina, *Inverse Problems and Applications*, Springer International Publishing, Switzerland, 2015.

[6] L. Beilina and M. Klibanov, *Approximate Global Convergence and Adaptivity for Coefficient Inverse Problems*, Springer, 2012.

[7] L. Beilina and E. Karchevskii, The layer-stripping algorithm for reconstruction of dielectrics in an optical fiber, Inverse Problems and Applications, *Springer Proceedings in Mathematics & Statistics*, **(120)**, 125–134 (2015).

[8] D. P. Bertsekas, *Constrained Optimization and Lagrange Multiplier Methods*, Athena Scientific, Belmont, Massachusetts, 1996.

[9] J. Brillet, *Manuel* MAPLE *9.5*, Lab. d'Astrophysique de Bordeaux, Université Bordeaux 1, France, 2007.

[10] E. K. P. Chong and S. H. Żak, *An Introduction to Optimization*, Wiley-Interscience, 2001.

[11] M. T. Chu and G. H. Golub, Strutured Inverse Eigenvalue Problems, *Acta Numer.*, 1–71 (2002).

[12] M. T. Chu and G. H. Golub, *Inverse Eigenvalue Problems*, Oxford University Press, Oxford, 2005.

[13] P. G. Ciarlet, *Introduction à l'Analyse Numérique Matricielle et à l'Optimisation*, Masson, 1988.

[14] C. M. DeCusatis and C. J. DeCusatis, *Fiber Optic Essentials*, Elsevier, 2006.

[15] R. Djellouli, *Contribution à l'Analyse Mathématique et au Calcul des Modes Guidés des Fibres Optiques*, Thèse de Doctorat es-Sciences, Université Paris-Sud, France, 1988.

[16] R. Djellouli, C. Bekkey, A. Choutri and H. Rezgui, A Local Boundary Condition Coupled to a Finite Element Method to Compute Guided Modes of Optical Fibers Under the Weak Guidance Assumptions, *Math. Method in Appl. Sci.*, **(23)**, 1551–1583 (2000).

[17] Y. Dodge, S. Gonano-Weber and J. P. Renfer, *Optimisation Appliquée*, Springer-Verlag, 2005.

[18] H. J. R. Dutton, *Understanding Optical Communications*, IBM, 1998.

[19] M. El Marraki, *Le Langage de Programmation* MAPLE, Université Mohammed V-Agdal, Faculté des Sciences, Rabat, 2007.

[20] W. A. Gambling, D. N. Payne, H. Matsumura and R. B. Dyott, Determination of Core Diameter and Refractive-index Difference of Single-mode Fibers by Observation of the Far-field Pattern, *Microwaves, Optics and Acoustics*, **1(1)**, 13–17 (1976).

[21] A. Ghatak and K. Thyagarajan, *Optical Waveguides and Fibers*, University of Connecticut, U.S.A., 2000.

[22] L. Guillopé, *Optimisation sous Contrainte*, Laboratoire de mathématiques Jean Leray, Département de mathématiques, UFR Sciences et techniques, Université de Nantes, 2014.

[23] F. Hartmann and C. Katz, *Structural Analysis with Finite Elements*, Springer-Verlag, 2007.

[24] J. B. Hiriart-Urruty, *Optimisation et Analyse Convexe*, EDP Sciences, France, 2009.

[25] F. Idachaba, D. U. Ike and O. Hope, *Future Trends in Fiber Optics Communication*, Proceedings of the World Congress on Engineering, Vol I, London, WCE, 2014.

[26] V. Isakov, *Inverse Problems for Partial Differential Equations*, Springer Science, 2006.

[27] G. Jomphe, *Introduction à* MAPLE, École Polytechnique de Montréal, 2001.

[28] E. M. Karchevskii, A. O. Spiridonov, A. I. Repina, and L. Beilina, Reconstruction of Dielectric Constants of Core and Cladding of Optical Fibers Using Propagation Constants Measurements, *Physics Research International*, Article ID 253435, (2014).

[29] E. M. Karchevskii, L. Beilina, A. O. Spiridonov and A. I. Repina, Reconstruction of Dielectric Constants of Multi-layered Optical Fibers Using Propagation Constants Measurements, **arXiv:1512.06764v1**, (2015).

[30] E. M. Karchevskii, A. O. Spiridonov and L. Beilina, Determination of Permittivity from Propagation Constant Measurements in Optical Fibers, *Physics Research International*, Springer Proceedings in Mathematics & Statistics, **(120)**, 55–66 (2015).

[31] A. V. Khomchenko, *Waveguide Spectroscopy of thin Films*, NY: Academic Press, 2005.

[32] J. Lafontaine, *Introduction aux Variétés Différentielles*, Presses Universitaires de Grenoble, 1996.

[33] R. H. Landau, *A First Course in Scientific Computing*, Princeton University Press, 2005.

[34] T. Lara, N. Merentes, E. Rosales and M. Valera, Some Characterizations of Strongly Convex Functions in Inner Product Spaces, *Mathematica Aeterna*, **6(4)**, 651–657 (2014).

[35] V. Manet, *La Méthode des Éléments Finis: Vulgarisation des Aspects Mathématiques. Illustration des Capacités de la Méthode*, DEA, Eléments finis pour l'ingénieur, ViM2, Lyon, 2013.

[36] D. Marcuse, *Theory of Dielectric Optical Waveguides*, Academic Press Inc., 1974.

[37] S. Mehellou and F. Rehouma, Détermination du Profil d'indice d'un Guide Optique Plan à Gradient d'indice, *Annales des Sciences et Technologie* (Algeria), **1(3)**, 70–81 (2011).

[38] T. Meis and U. Marcowitz, *Numerical Solution of Partial Differential Equations*, Springer-Verlag, New York Inc., 1981.

[39] H. Murata, *Handbook of Optical fibers and Cables*, Marcel Dekker, New York, 1988.

[40] F. D. M. Neto and A. J. S. Neto, *An Introduction to Inverse Problems with Applications*, Springer-Verlag, 2013.

[41] J. Nunemacher, Lagrange Multipliers Can Fail To Determine Extrema, *College Math. J.*, **1(34)**, 60–62 (2003).

[42] K. Okamoto, *Fundamentals of Optical Waveguides*, Elsevier, U.S.A., 2006.

[43] H. Oudin, *Méthode des Éléments Finis*, École d'ingénieurs. Nantes, France, 2008.

[44] C. Planiden and X. Wang, Strongly Convex Functions, Moreau Envelopes and the Generic Nature of Convex Functions with Strong Minimizers, **arXiv:1507.07144v1 [math.OC]**, 1–25 (2015).

[45] C. Poulin, MAPLE, Groupe de réflexion NOUMEA, 2010.

[46] J. Powers, *An Introduction to Fiber Optic Systems*, Mc Graw-Hill, 1986.

[47] J. P. Préaux, *Optimisation continue*, Aix-Marseille Université, France, 2010.

[48] H. Rezgui, *Une Méthode d'Éléments Finis Couplée à une Condition Artificielle pour le Calcul des Modes Guidés dans les Fibres Optiques en Régime de Faible Guidage*, Thèse de Magistère, ENS de Kouba, Algérie, 1999.

[49] H. Rezgui and A. Choutri, *An Inverse Eigenvalue Problem. Application: Graded-Index Optical Fibers*, Opt. Quant. Electron., **49(10)**, (2017):
https://link.springer.com/article/10.1007/s11082-017-1154-9.

[50] R. T. Rockafellar, Lagrange Multipliers and Optimality, *SIAM Rev.*, **(32)**, 183–238 (1993).

[51] C. T. F. Ross, *Advanced Finite Element Methods*, Horwood Publishing, 1998.

[52] J. K. Shaw, *Mathematical Principles of Optical Fiber Communications*, Siam, 2004.

[53] F. M. E. Sladen, D. N. Payne and M. J. Adams, Determination of Optical Fiber Refractive Index Profiles by a Near-field Scanning Technique, *Appl. Phys. Lett.*, **5(28)**, 255–258 (1976).

[54] V. I. Sokolov et al., Investigation of optical properties of multilayer dielectric structures using prism-coupling technique, *Quantum Electron.*, **9(45)**, 868–872 (2015).

[55] A.B. Sotsky et al., Waveguide spectroscopy of bilayer structures, *Tech. Phys.*, **60(8)**, 1220–1226 (2015).

[56] W. F. Trench, *The Method of Lagrange Multipliers*, Department of Mathematics, Trinity University, San Antonio, Texas, U.S.A., 2013.

[57] K. Thyagarajan and A. Ghatak, *Fiber Optic Essentials*, Wiley, 2007.

[58] R. Tyrrell Rockafellar, Lagrange Multipliers and Optimality, *Siam Rev.*, **(32)**, 183–238 (1993).

[59] D. Verwærde and P. Laurent-Gengoux, *Optimisation*, École Centrale, Paris, 2007.

[60] M. Willem, *Analyse Convexe et Optimisation*, Ciaco, 1987.

[61] O. Ziemann, J. Krauser, P. E. Zamzow and W. Daum, *Optical Short Range Transmission Systems*, Hardcover, 2008.

Author information

Hayat REZGUI and Abdelaziz CHOUTRI, Département de Mathématiques, École Normale Supérieure de Kouba, B.P. 92, Vieux Kouba, 16038, Algiers, Algeria.
E-mail: rezguihayat@yahoo.fr

Received: February 11, 2017.

Accepted: May 28, 2017.